Effect of Antimicrobial Peptides from Australian Tree Frogs on Anionic Phospholipid Membranes[†]

John D. Gehman,[‡] Fiona Luc,[‡] Kristopher Hall,[§] Tzong-Hsien Lee,[§] Martin P. Boland,[‡] Tara L. Pukala,[∥] John H. Bowie,[∥] Marie-Isabel Aguilar,[§] and Frances Separovic*[,‡]

School of Chemistry, University of Melbourne, Melbourne, VIC 3010, Australia, Department of Biochemistry and Molecular Biology, Monash University, Melbourne, VIC 3800, Australia, and Department of Chemistry, University of Adelaide, Adelaide, SA 5005, Australia

Received February 26, 2008; Revised Manuscript Received June 7, 2008

ABSTRACT: Skin secretions of numerous Australian tree frogs contain antimicrobial peptides that form part of the host defense mechanism against bacterial infection. The mode of action of these antibiotics is thought to be lysis of infectious organisms via cell membrane disruption, on the basis of vesicle-encapsulated dye leakage data [Ambroggio et al. (2005) *Biophys. J. 89*, 1874−1881]. A detailed understanding of the interaction of these peptides with bacterial membranes at a molecular level, however, is critical to their development as novel antibacterial therapeutics. We focus on four of these peptides, aurein 1.2, citropin 1.1, maculatin 1.1, and caerin 1.1, which exist as random coil in aqueous solution but have α-helical secondary structure in membrane mimetic environments. In our earlier solid-state NMR studies, only neutral bilayers of the zwitterionic phospholipid dimyristoylphosphatidylcholine (DMPC) were used. Deuterated DMPC (d_{54}-DMPC) was used to probe the effect of the peptides on the order of the lipid acyl chains and dynamics of the phospholipid headgroups by deuterium and ^{31}P NMR, respectively. In this report we demonstrate several important differences when anionic phospholipid is included in model membranes. Peptide−membrane interactions were characterized using surface plasmon resonance (SPR) spectroscopy and solid-state nuclear magnetic resonance (NMR) spectroscopy. Changes in phospholipid motions and membrane binding information provided additional insight into the action of these antimicrobial peptides. While this set of peptides has significant C- and N-terminal sequence homology, they vary in their mode of membrane interaction. The longer peptides caerin and maculatin exhibited properties that were consistent with transmembrane insertion while citropin and aurein demonstrated membrane disruptive mechanisms. Moreover, aurein was unique with greater perturbation of neutral versus anionic membranes. The results are consistent with a surface interaction for aurein 1.2 and pore formation rather than membrane lysis by the longer peptides.

Antibacterial peptides are widely distributed in nature with several hundred antimicrobial peptides characterized to date, and their sequences are available together with a comprehensive list of reviews and publications (*1*–*3*). The majority of antibacterial peptides appear to act by permeabilisation of the target membrane (*4*–*6*), which could lead to their development as novel therapeutic agents, in particular, those that preferentially lyse bacterial cell membranes. Therefore, understanding the mechanistic properties of antibacterial peptides and the factors that govern selectivity is of considerable interest.

The most abundant and well-studied antibacterial peptides are linear helical peptides, which are generally short (<40 residues), cationic, and adopt amphipathic α-helical structures in membrane environments, e.g., cecropins, magainins, and melittin (*7*). Several models have been proposed to describe how these helical peptides disrupt bacterial membranes, of which the "pore" and "surface interaction" mechanisms are the most common. In the barrel-stave model of the pore mechanism, peptides aggregate at the membrane surface before inserting into the membrane and forming a transmembrane pore (*6, 8*). An alternative to the barrel-stave model, where the lumen of the pore is lined by the peptides, is the "toroidal pore" where both peptides and the phospholipid headgroups line the pore (*9, 10*). The carpet model is an example of a surface interaction mechanism where peptides assemble parallel to the membrane surface and form a detergent-like monolayer (*5, 6*). Notwithstanding the mode of action, ultimately the disruption of normal membrane function results in cell lysis.

The skin secretions of numerous Australian tree frogs contain antimicrobial peptides (AMP),[1] which cause cell lysis

[†] The authors thank the Australian Research Council for the financial support of this project.

* To whom correspondence should be addressed. Tel: +61 3 8344 2447. Fax: +61 3 9347 5180. E-mail: fs@unimelb.edu.au.

[‡] University of Melbourne.

[§] Monash University.

[∥] University of Adelaide.

[1] Abbreviations: AMP, antimicrobial peptides; CHAPS, 3-[(cholamidopropyl)dimethylammonio]-1-propanesulfonate; CSA, chemical shift anisotropy; DMPC, 1,2-dimyristoyl-*sn*-glycero-3-phosphocholine; DMPG, 1,2-dimyristoyl-*sn*-glycero-3-[phospho-*rac*-(1-glycerol)]; DPC, dodecylphosphatidylcholine; MAS, magic angle spinning; MIC, minimum inhibitory concentration; MLV, multilamellar vesicle; MOPS, 3-(*N*-morpholino)propanesulfonic acid; NMR, nuclear magnetic resonance; PC, phosphatidylcholine; PG, phospho-*rac*-(1-glycerol); SPR, surface plasmon resonance; TFE, trifluoroethanol.

10.1021/bi800320v CCC: $40.75
Published on Web 07/25/2008

Table 1: Amino Acid Sequence of Antibacterial Peptides from Australian Tree Frogs (*11, 12*) Used in This Study[a]

peptide	amino acid sequence	MW	AA	net charge
aurein 1.2	GLFDII----KKIA--------ESF-NH_2	1478	13	+1
citropin 1.1	GLFDVI----KKVA-SVI----GGL-NH_2	1613	16	+2
maculatin 1.1	GLFGVL---AK-VAAHVVPAIAEHF-NH_2	2145	21	+3
caerin 1.1	GLLSVLGSVAKHVLPHVVPVIAEHL-NH_2	2582	25	+4

[a] Approximate alignments highlight potential structural or mechanistic determinants. Nonhydrophobic residues (except glycine) are underlined.

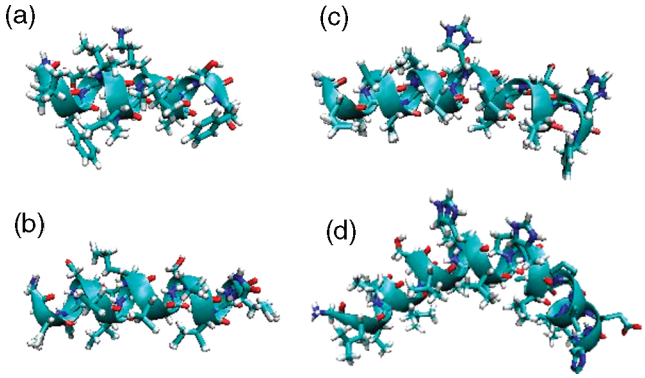

FIGURE 1: NMR-derived structures of selected antimicrobial frog peptides in TFE/water: (a) aurein 1.2, (b) citropin 1.1, (c) maculatin 1.1, and (d) caerin 1.1 (*11, 13*).

(*11*). We have chosen to study the peptides aurein 1.2 (13 residues), citropin 1.1 (16 residues), maculatin 1.1 (21 residues), and caerin 1.1 (25 residues), which have potential applications in the fight against bacterial infection. These peptides are unstructured in water and form amphipathic α-helical structures in trifluoroethanol (TFE)/water, in dodecylphosphocholine micelles, and with phosphatidylcholine (PC) vesicles (*11–14*). The sequences and structures of the peptides are shown in Table 1 and Figure 1. These peptides are effective against a range of Gram-positive bacteria, including pathogenic species, and cause disruption of bacterial cell membranes (*15*).

The longer peptides, maculatin and caerin, are capable in principle of inserting into the membrane with transmembrane orientation, as their membrane-induced α-helical lengths are long enough to span the bilayer (*11, 13*). These peptides have one and two proline residues, respectively, which create a kink in the structure, and may be crucial to membrane interaction. By contrast, aurein and citropin are too short to span a bilayer and thus are more likely to have a surface orientation or partially insert (*11, 12, 16*) and act as a detergent to disrupt the membrane (*12*).

Model membrane systems have been used to study the effects of these cationic AMP from amphibians (*11, 12, 14, 16–20*). In our earlier solid-state NMR studies (*14, 16*), neutral bilayers of the zwitterionic phospholipid dimyristoylphosphatidylcholine (DMPC) were used. Deuterated DMPC (d_{54}-DMPC) was used to probe the effect of the peptides on the order of the lipid acyl chains and dynamics of the phospholipid headgroups by deuterium and ^{31}P NMR, respectively. In this report we demonstrate several important differences when anionic phospholipid is included in model membranes. The net negative charge introduced at the vesicle surface by incorporation of dimyristoylphosphatidylglycerol (DMPG) with DMPC better mimics the electrostatics of negatively charged bacterial membranes (*21*) in contrast to eukaryotic cells, which could clearly be an important aspect of cationic antibacterial peptides selectivity. In this study, we report how these AMPS interact with anionic membranes of DMPC/DMPG (2:1) using solid-state NMR and surface plasmon resonance (SPR) spectroscopy (*22*) to characterize peptide−membrane interactions. The peptide concentrations used for NMR were high, equivalent to our earlier work using neutral bilayers for which little effect was observed, while the concentrations used for SPR were chosen to be in the range that kills bacteria and lyses model membranes. The combination of solid-state NMR and SPR techniques as applied here to model membrane bilayers provides insight into the mechanism by which AMP interacts with the bacterial membrane.

MATERIALS AND METHODS

Preparation of Phospholipid NMR Samples. DMPC, d_{54}-DMPC, and DMPG, were purchased from Avanti Polar Lipids (Alabaster, AL) and used without further purification. Two lipid systems were prepared: a pure DMPC lipid system (DMPC/d_{54}-DMPC, 1:1 mol ratio) and a mixed lipid system (DMPC/d_{54}-DMPC/DMPG, 1:1:1 mol ratio). Phospholipids were dissolved in ~1 mL of chloroform/methanol (9:1), and a rotary evaporator was used to form a thin film on a 50 mL round-bottom flask. Samples were placed at high vacuum overnight to remove any trace amounts of solvent.

Preparation of Peptide−Lipid NMR Samples. Peptides were purchased from Mimotopes Ltd. (Melbourne, Australia) with the purity of >90% and used without additional purification. The peptides, aurein 1.2 (0.7 mg), citropin 1.1 (0.8 mg), maculatin 1.1 (1.02 mg), and caerin 1.1 (1.2 mg), were dissolved in 75 μL of 10 mM 3-(*N*-morpholino)propanesulfonic acid (MOPS) buffer and vortex mixed to assist solubility. Salt was not included in the buffer to minimize electric field heating effects under RF pulsing during subsequent NMR experiments. The peptide−buffer solutions were used to hydrate dried lipid mixtures to a final 10:1 lipid/peptide molar ratio. Upon complete suspension of lipid, the peptide−lipid mixture was submitted to five cycles of freeze−thaw, centrifuged, and transferred to a 5 mm NMR rotor.

Solid-State NMR Experiments. SS-NMR experiments were performed on a Varian (Palo Alto, CA) Inova-300 spectrometer using a 5 mm HX AutoMAS (Varian) probe. Static ^{2}H and ^{31}P spectra were collected at 30 °C for each of the peptides in the different lipid compositions. Static deuterium spectra were carried out 46.09 MHz using a quadrupolar-echo pulse sequence (*23*). The operating parameters included 3.8 μs 90° pulses, 40 μs echo delay, and 0.5 s recycle delay. Spectra were collected with an incomplete final echo delay and 500 kHz spectral width such that left shifting followed by downsampling allowed for Fourier transformation at the top of the echo. Typically 120K scans were collected, and 100 Hz exponential line broadening was applied. "De-

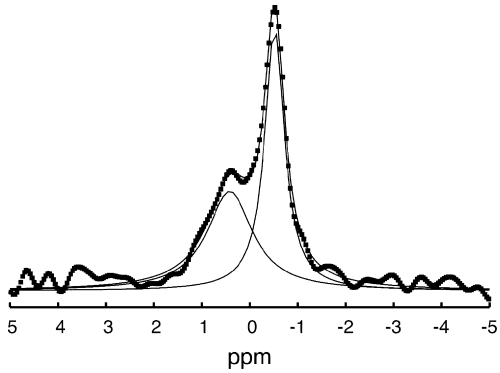

FIGURE 2: ^{31}P MAS NMR spectrum of DMPC/DMPG (2:1) bilayers with aurein 1.2. The filled squares are the experimental data, and the solid lines are two Lorentzian functions that are summed to give the line shape and used to determine the peak intensities.

Pakeing" of deuterium spectra and calculation of order parameters was performed as previously described (*24, 25*).

Static ^{31}P NMR spectra were collected at 121.5 MHz using a Hahn echo sequence pulse with proton decoupling to allow for correct preacquistion delays, which obviates the need to set nonzero linear phase corrections. The operating parameters were 5.8 μs 90° pulse followed by a 62 μs total Hahn echo time, and 12K scans were acquired and processed with 100 Hz exponential line broadening.^{31}P relaxation experiments were carried out under magic angle spinning (MAS) (*26, 27*) at 6.25 kHz. T_1 relaxation times were measured using the inversion recovery pulse sequence with a recycle delay of 4 s and variable delay (τ) values between 0.03 and 3.5 s. T_2 relaxation times were measured with a Hahn spin−echo experiment with total echo delay (τ) values between 0.64 and 24 ms using integer multiples of the rotor period.

Relaxation times in the pure DMPC system were found by fitting peak intensities to single exponential equations using Gnuplot (*28*). Two overlapping peaks in the DMPC/DMPG mixed system were deconvoluted using Gnuplot (*28*) by fitting the spectra to a sum of two Lorentzian lines of the form

$$f(\nu) = \Sigma_i \frac{A_i}{1.0 + \left[\frac{2(\nu - \mu_i)}{\Delta_i}\right]^2}$$

where A_i is the maximum amplitude, ν is spectral frequency, μ_i is the center of the Lorentzian line, and Δ_i is the full-width half-maximum of the component. The values of μ_i and Δ_i were fixed for each sample following inspection of the spectra from the shortest echo time in the T_2 experiment and the shortest and longest relaxation delays in the T_1 experiment. The optimized maximum amplitudes A_i of the individual "major" and "minor" peak components (Figure 2) for each delay time were individually fit to single exponential decays to determine relaxation times for the two components that comprise the signal.

Preparation of SPR Samples. DMPC was dissolved in chloroform, and DMPG was dissolved in a mixture of chloroform/methanol (3:1 v/v) to create individual stock solutions of 5 mM. These stock solutions were then aliquoted out in the desired ratios: DMPC and DMPC/DMPG (2:1 v/v) into clean tubes. The solvent was then evaporated under a gentle stream of N_2 and vacuum desiccated overnight. Prior to experiments, lipids were resuspended in 10 mM MOPS buffer (pH 6.9) with 150 mM NaCl (*29*) and vortexed to give a concentration of 1 mM. The resultant lipid dispersion was then sonicated with a bath-type sonicator until clear. The lipid solutions were extruded through a 50 nm pore diameter polycarbonate membrane to form the appropriate size liposomes for the sensor chip. Peptide solutions (0.1 mM) were prepared by dissolving aurein 1.2, citropin 1.1, maculatin 1.1, and caerin 1.1 in 10 mM MOPS plus 150 mM NaCl buffer. These solutions were sonicated to assist solubility and then filtered and diluted to 1, 5, 10, and 20 μM.

Table 2: Effect of Peptides on ^{2}H Quadrupolar Splitting of DMPC and DMPC/DMPG Bilayers

DMPC			DMPC/DMPG (2:1)		
peptide	CD_2 (kHz)	CD_3 (kHz)	peptide	CD_2 (kHz)	CD_3 (kHz)
control	29.9	3.8	control	27.1	3.2
aurein 1.2	30.3	4.1	aurein 1.2	29.2	3.4
citropin 1.1	28.6	3.8	citropin 1.1	29.9	3.8
maculatin 1.1	30.1	3.8	maculatin 1.1	29.9	3.8
caerin 1.1	29.9	3.9	caerin 1.1	29.2	3.6

SPR Experiments. SPR experiments were carried out with a Biacore T100 analytical system with on L1 sensor chip (Biacore, Uppsala, Sweden). The system was cleaned using the "desorb and sanitize" protocol with a maintenance chip and then allowed to run overnight with water. The L1 chip was docked and first washed with an injection of 5 μL of 20 mM nonionic detergent, 3-[(cholamidopropyl)dimethylammonio]-1-propanesulfonate (CHAPS), at a flow rate of 5 μL/min to clean the chip surface. The extruded lipid solutions were then applied to all four flow cells on the chip surface simultaneously with injections of 80 μL at a low flow rate of 2 μL/min. To remove any mutilamellar structures from the lipid surface and to stabilize the baseline, 30 μL of 10 mM NaOH was injected at 50 μL/min. The peptide solution (100 μL) was then injected onto the model membrane surface at a flow rate of 30 μL/min, having a total injection time of 200 s. On completion of injection, buffer flow continued to allow a dissociation time of 600 s. CHAPS was then injected (5 μL at 5 μL/min) to clear the chip of any material. All binding experiments were carried out at 30 °C. All solutions were freshly prepared, degassed, and filtered through a 0.2 μm filter. Each sample was run in duplicate.

RESULTS

^{31}P and ^{2}H solid-state NMR techniques have been applied to investigate the interaction between AMP and bilayer membranes (*7, 30, 31*) and were used to probe changes in phospholipid motion and conformation over a range of time scales.

^{2}H Static Solid-State NMR. ^{2}H NMR experiments were performed to determine if the peptides disrupted the lipid acyl chains, where an increase in quadrupole splitting indicates an increase in acyl chain order. The outermost splitting of the 90° edge for the CD_2 of pure DMPC bilayers was 29.9 ± 0.1 and 3.8 ± 0.1 kHz for CD_3. DMPC samples with peptide showed little change in splitting, with the exception of citropin (Table 2), where the CD_2 splitting decreased slightly, indicating that citropin 1.1 disordered the acyl chains of the bilayer but not the terminal methyl. Aurein

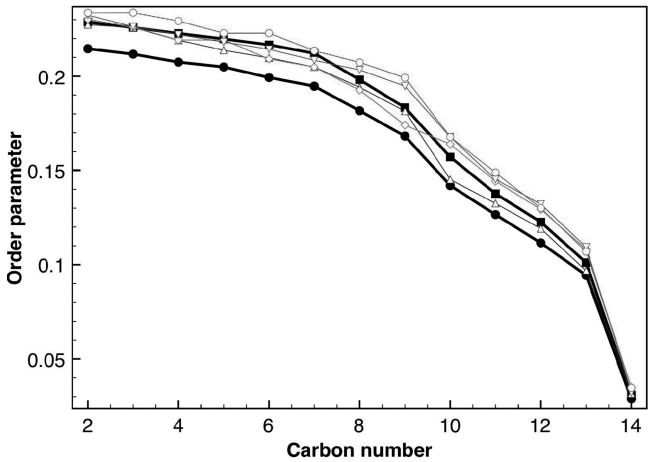

FIGURE 3: Order parameters of the ^{2}H acyl chains in DMPC bilayers (■) and DMPC/DMPG bilayers (●) with aurein (Δ), citropin (◇), maculatin (▽), and caerin (○).

1.2, maculatin 1.1, and caerin 1.1 showed little change in the CD_2 and CD_3 splitting, which indicated weak interaction with the neutral phospholipid membranes.

Deuterium NMR spectra of perdeuterated lipid acyl chains produce a complex line shape, the sum of individual Pake powder patterns from each CD_n position (*26, 27, 32, 33*). "De-Pakeing" of the spectrum (*23*) derives a measure of the segmental dynamics or the order parameter profile for all CD_n positions down the acyl chain and may reveal changes in the membrane structure and dynamics upon the introduction of peptide. Acyl chain order parameters in the pure DMPC lipid system control were 0.23 at the CD_2 closest to the membrane surface and 0.03 at the terminal CD_3 in the membrane interior (Figure 3). All four peptides had little impact on these order parameters. In the DMPC/DMPG (2:1) lipid system, the PG headgroup decreased the DMPC acyl chain order by 9% at the CD_2 closest to the surface and 22% at the terminal CD_3. Each of the peptides increased the deuterated DMPC acyl chain order within the mixed lipid system to a state similar to that in the pure DMPC control vesicles, albeit less so for aurein 1.2 particularly at the terminal CD_3. Full order parameter profiles (Figure 3) indicate that the DMPC ordering effect of citropin 1.1, maculatin 1.1, and caerin 1.1 in DMPC/DMPG extends through the full length of the chain. Aurein, however, appeared to significantly order DMPC in the mixed lipid system only down through C_9 of the acyl chain. The ordering effect of the peptides on DMPC in the mixed lipid system, however, may be indirect: by taking a truly mixed lipid system and actively segregating DMPG out of the mixture, DMPC-enriched domains could be formed which experience similar fluctuations to pure DMPC.

^{31}P Static NMR. Static ^{31}P NMR of unoriented phospholipid liposomes results in a powder pattern with a chemical shift anisotropy (CSA). In liquid-lamellar phase membranes, due to fast axial rotation of lipids, the CSA is axially symmetric with an overall width that depends on the ^{31}P headgroup orientation and disorder (*33–38*). The static ^{31}P line shape, therefore, is used to probe perturbations to headgroup orientation and dynamics on the 10^{-4} s time scale. The ^{31}P static powder patterns of DMPC bilayers showed a significant drop of 4−10 ppm in CSA with the addition of all peptides (Table 3). The decrease in CSA indicates that

Table 3: Effect of Peptides on ^{31}P CSA of DMPC and DMPC/DMPG Bilayers

peptide	DMPC ^{31}P CSA (ppm)	peptide	DMPC/DMPG (2:1) ^{31}P CSA (ppm)
control	47.9	control	41.5
aurein 1.2	40.6	aurein 1.2	40.3
citropin 1.1	37.8	citropin 1.1	38.1
maculatin 1.1	37.8	maculatin 1.1	40.2
caerin 1.1	43.8	caerin 1.1	39.9

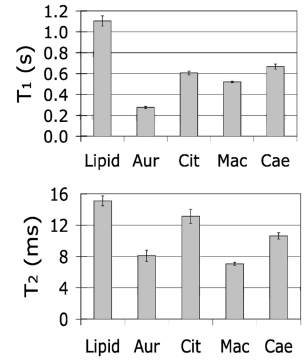

FIGURE 4: Effect of peptide addition on ^{31}P relaxation times: (a, top) T_1 and (b, bottom) T_2 of DMPC bilayers. The error bars represent the range of values calculated using Gnuplot (*28*).

the peptides are disordering the DMPC headgroups and/or altering their orientation, with caerin 1.1 having the least effect. In the DMPC/DMPG (2:1) lipid system, the CSA widths in Table 3 are an aggregate of both DMPC and DMPG; the PG headgroup decreased the overall CSA width by 13% relative to pure DMPC. This corresponds to a headgroup orientation more parallel to the bilayer in the presence of PG and/or an increase in headgroup disorder on the $\sim 10^{-4}$ s time scale to complement the disorder noted above for the acyl chains on the $\sim 10^{-5}$ s time scale. In contrast to the pure DMPC system, the peptides had only slight further influence on headgroup conformation and/or disordering effect for the DMPC/DMPG bilayers.

^{31}P Relaxation Studies. Measurement of ^{31}P T_1 and T_2 relaxation times are used to characterize intensity of fluctuations on the fast (10^{-9} s) and slow (10^{-3} s) time scales, respectively (*39–41*). Changes in T_1 upon addition of AMP indicate changes in individual lipid dynamics, whereas changes to T_2 indicate changes in collective membrane motions. In pure DMPC lipid systems, all peptides increased dynamics on both the 10^{-9} and 10^{-3} s time scales, dominated by fast fluctuations of individual lipid headgroups and slow fluctuations of the anisotropic chemical shift tensor under collective bilayer motions, respectively. Figure 4a shows that citropin 1.1, maculatin 1.1, and caerin 1.1 had similar effects on the fast lipid motions (decrease in T_1), but aurein 1.2 had even more effect, indicating that it may interact with neutral bilayers in a different manner to the other peptides. Figure 4b indicates that both aurein 1.2 and maculatin 1.1 increased collective bilayer motions to a similar extent, roughly halving the T_2 relaxation time, while citropin 1.1 and caerin 1.1 had less effect on these dynamics.

The ^{31}P MAS spectra revealed two components from the DMPC/DMPG (2:1) samples (Figure 2). Several aspects of these experiments suggest that the major peak corresponds to DMPC and the minor to DMPG: the major and minor peaks were upfield and downfield of 0 ppm, respectively (*24*);

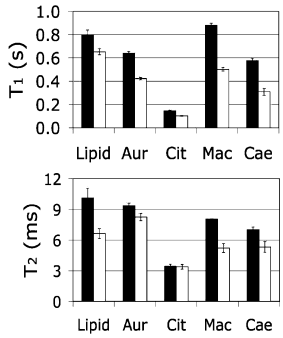

FIGURE 5: Effect of peptide on ^{31}P relaxation times of DMPC (black) and DMPG (white): (a, top) T_1 and (b, bottom) T_2 in DMPC/DMPG bilayers. The error bars represent the range of values calculated using Gnuplot (*28*).

deconvolution of major and minor components indicates that they were present in approximately 2:1 proportion; and the intensities of each peak fit well to single exponential curves in both T_1 and T_2 experiments. The peptides affected each phospholipid component within the mixed membrane system to different degrees. The AMP generally decreased both T_1 and T_2 relaxation times of both DMPC and DMPG, indicating a general tendency to influence lipid and membrane dynamic modes such that fluctuations increase on both fast and slow time scales. Most notable is the dramatic reduction in T_1 and T_2 for both lipid components by citropin 1.1 (Figure 5). An interesting exception to the trend is maculatin 1.1 with an increase in T_1 by about 10% for the major lipid component, i.e., an apparent reduction in intensity of fast motions for DMPC headgroups, while displaying an increase in fast fluctuations for the DMPG headgroups. Both aurein 1.2 and caerin 1.1 affected phospholipid motions but not to the extent of citropin 1.2 and, like maculatin 1.1, indicated a preferential interaction with the anionic lipid.

Surface Plasmon Resonance Spectroscopy. SPR spectroscopy is a mass sensitive technique that measures the change of adsorbed mass at the sensor surface in real time (*22, 42*). Changes in mass are detected on a gold-coated surface of a sensor chip by changes in the refractive index of the reflected polarized light, which is shone onto the gold surface. The vesicle capture sensor chip has dextran modified matrix molecules on the surface that allow binding of liposomes (*22*) to mimic a fluid bilayer membrane. A change in the refractive index due to material being added or removed from the chip is proportional to the change in mass, which results in a sensorgram of response units (RU) versus time. A typical sensorgram shows a response, which increases and reaches a plateau some point after injection and decreases quite rapidly after the chip is washed to remove material. SPR sensorgrams can show the strength of association and dissociation on the chip surface of AMPs (*22*).

SPR of DMPC Bilayers. The peptides were introduced to the two lipid systems at concentrations of 1, 5, 10, and 20 μM, with the higher concentrations similar to the reported minimum inhibitory concentration (MIC) against bacteria (*11*). The sensorgrams of each peptide binding to the pure DMPC lipid system are shown in Figure 6 and indicate that each of the peptides demonstrated rapid initial binding to the model membrane.

In addition, the response was also proportional to peptide concentration with one exception. At the highest concentration, a sharp drop in response occurred soon after the introduction of aurein 1.2, which was followed by a sharp drop again at the end of the association phase. The abrupt drop in response (approximately 3500 RU) after the association to RU below the original baseline indicates loss of membrane material from the surface and demonstrates that aurein 1.2 rapidly bound and ruptured the membrane which was then stripped off the surface of the L1 chip. The lower concentrations did not show such a dramatic effect but appeared also to exhibit some lipid dissociation simultaneous with peptide association. Regardless of concentration, aurein 1.2 displayed strong interactions and significant lysis or loss of DMPC bilayers.

The sensorgrams of citropin 1.1 with DMPC gave prototypical curves, with the response proportional to peptide concentration (4300 maximum RU). While citropin 1.1 appeared to bind very strongly to the membrane, with a significant amount of peptide still bound to the membrane in the dissociation phase, no loss of bilayer was evident.

The profile of the maculatin−DMPC sensorgrams during association indicates that maculatin 1.1 did not disrupt the bilayer to any significant extent. While the 20 μM sample had a RU of 2000, there was a gradual drop in RU at 5 and 10 μM. The dissociation phase showed a short immediate drop in material followed by rapid decline toward baseline, indicating that a small amount of material was being taken off the membrane. The differences in the curves indicate that the binding mechanism of this peptide is dependent on concentration.

The caerin−DMPC sensorgram showed a similar degree of binding to that observed for maculatin 1.1, with a comparable maximum response of ~2400 RU at 20 μM. The effect of caerin 1.1 was also concentration dependent but not linearly proportional to concentration and suggests the binding was approaching saturation at 20 μM. Caerin appeared to behave similar to maculatin 1.1 and did not fundamentally disrupt bilayer integrity as lipid mass was not clearly stripped from the L1 surface.

SPR of DMPC/DMPG Bilayers. The sensorgrams showing the binding of peptides to the mixed DMPC/DMPG lipid system are shown in Figure 7. Aurein 1.2 had a similar affect on the DMPC/DMPG membrane as for the pure DMPC system, but the association response (4200 RU) was higher. In DMPC with aurein, lipid mass appears to be lost with a very fast initial drop in RU at 20 μM, whereas this effect was seen in the mixed bilayers at 10 μM and not 20 μM. This suggests that aurein 1.2 may have a preference for a negatively charged environment. Rupturing or loss of the membrane occurred almost immediately after peptide introduction into the flow cell.

There was a lower response of citropin 1.1 with DMPC/DMPG (2500 RU) in comparison to the DMPC system (4300 RU), and binding is related to concentration. However, there was a significant degree of peptide that remained bound to the membrane after washing, and the orientation of this strongly bound citropin is such that it does not cause rupturing of the membrane.

The sensorgrams show that, for maculatin 1.1 with DMPC/DMPG, the binding step competes with a partial rupturing process of the membrane. Maculatin 1.1 may have an optimum range for lytic activity, as it appeared to affect the membrane to a similar extent in the 5−10 μM range. Material was removed from the chip surface after a maximum

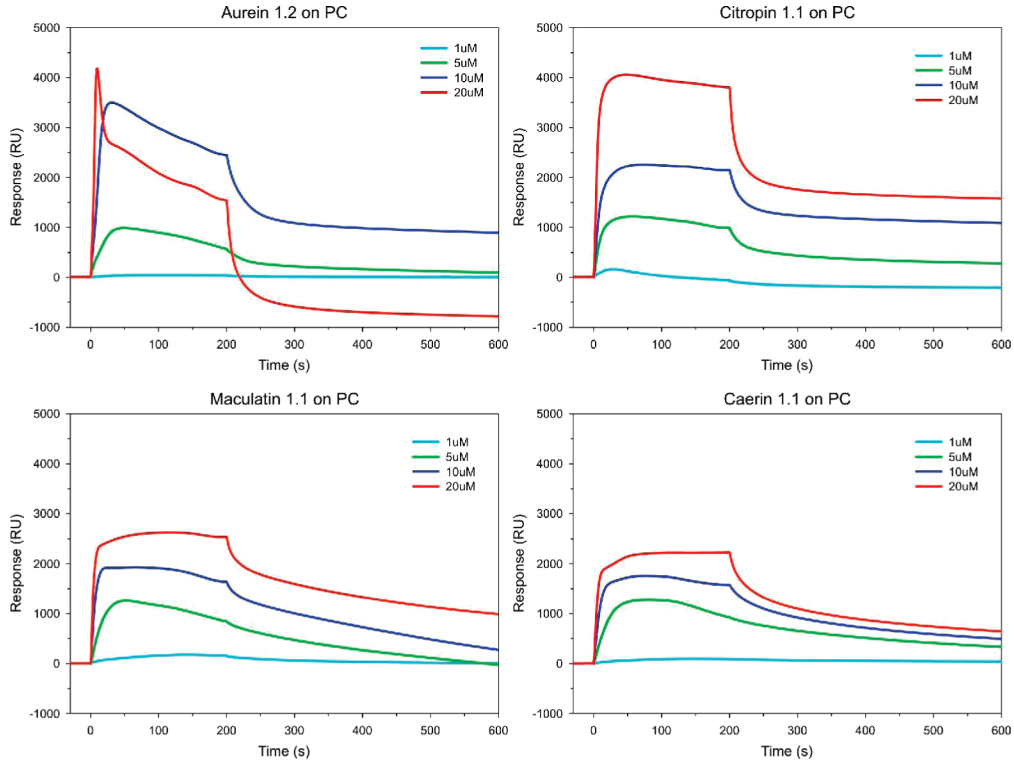

FIGURE 6: SPR sensorgrams of the peptide interactions with the DMPC membrane system.

association response of 2000 RU, which was the same as for DMPC. Comparison of the interaction of the peptide in the two different lipid systems demonstrates a preference for DMPG since maculatin led to greater disruption of the mixed lipid system.

Like maculatin, caerin 1.1 had a similar response value for both the DMPC and DMPC/DMPG systems (2000 RU) with less difference in the peptide interactions between the two lipid systems. However, in contrast to maculatin, caerin 1.1 did not show any evidence of membrane rupture, and the binding approached saturation at 20 μM. A significant amount of peptide remained associated with the bilayer following the wash, which suggests that caerin 1.1 embeds in the bilayer in such a way that does not destroy the membrane.

DISCUSSION

Antimicrobial peptides derived from the skin secretions of Australian tree frogs may provide valuable leads as a new class of antibiotics against infectious microbes based upon selectivity of prokaryotic versus mammalian cell membranes. Previous studies (*11*) have shown that aurein 1.2, citropin 1.1, maculatin 1.1, and caerin 1.1 are effective against Gram-positive bacteria and are only weakly hemolytic.

The sequence of each peptide is amphipathic and with a pattern which places hydrophilic residues roughly along a common face of a helix (Table 1). Approximate alignment of these four peptides indicates homology at the N-terminus, middle, and C-terminus of the peptides, with insertion of roughly one additional helical turn on going from aurein to citropin to maculatin to caerin. The persistence of the amphipathic pattern suggests that all four peptides may interact with membranes in the interfacial region at the bilayer surface. The rough conservation of register between homologous sequence regions in each of the four peptides further suggests that these common regions may be the determinants that govern a common topology and membrane-disruptive mechanism.

With the additional helical turns relative to aurein and citropin, maculatin and caerin become in principle long enough to span a membrane bilayer, which must also, therefore, be considered. Some sequence characteristics of maculatin 1.1 and caerin 1.1, however, argue against the proposition that these peptides adopt a transmembrane topology. First, the kink introduced by prolines in the α-helical structure of maculatin 1.1 in 50% TFE (*43*), and caerin 1.1 in 50% TFE (*44*) and DPC micelles (*45*), is energetically costly owing to the disruption in hydrogen bonding (*46*) known to be critical in stable transmembrane α-helical structure. Proline, though, is common in transmembrane helices: of 199 transmembrane helices known to high resolution, only one was found not to contain proline (*46*); and 47% of the 13606 putative α-helical transmembrane segments included in the homology-purged, single and multispan TMSTAT database (*47*) have one or more prolines. Second, there is a high prevalence of β-branched residues, which are typically thought to have greater propensity for β-sheet than for α-helix owing to the entropic cost of restricting the side chains to a single favorable rotamer position in a helix. Nevertheless, there is also a statistically significant overrepresentation of the βxxxβ motif (β = Ile or Val) in the TMSTAT database. One explanation is that the entropic cost paid to fix the rotamer conformations of β-branched residues upon folding of the helix encourages intermolecular association, as there is little further entropic cost associated with packing side chains across an interface (*47*). For maculatin 1.1 and caerin 1.1, such intermolecular association could result in a transmembrane oligomer, possibly forming a pore.

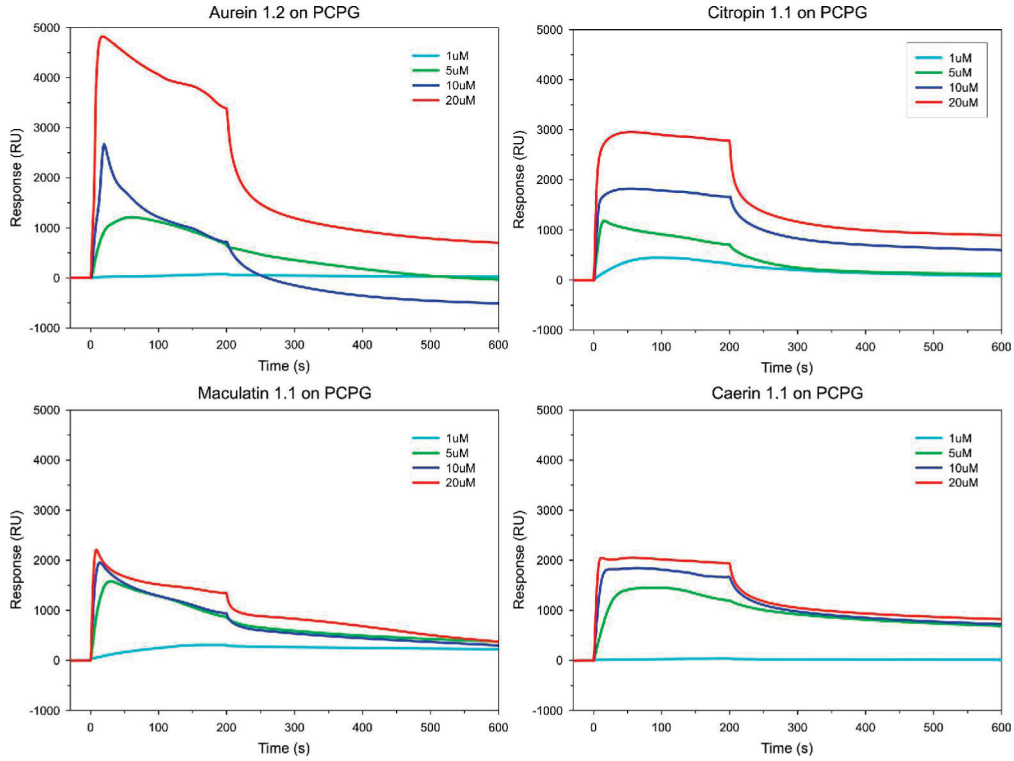

FIGURE 7: SPR sensorgrams of the peptide interaction with DMPC/DMPG membrane systems.

Our investigations provide evidence for the specific molecular basis of the bilayer interactions for each peptide to discriminate between the possible modes of membrane interaction and disruption, using SS NMR and SPR. We note, however, that low salt concentrations increase the electrostatic component of the interactions and so differences in apparent affinity between the NMR (low salt) and SPR (150 mM NaCl) experiments will be observed. However, the relative membrane affinity of each peptide was similar at the peptide concentrations used so that comparison of the peptides can be made.

Aurein 1.2. In a pure DMPC lipid system, aurein had little effect on lipid acyl chains (Table 2) but increased ^{31}P headgroup disorder on the 10^{-4} s time scale and/or caused the ^{31}P headgroup to lie more parallel to the bilayer surface (Table 3). Phospholipid dynamics on the 10^{-9} s time scale were substantially intensified, with increased fluctuations on the 10^{-3} s time scale also (Figure 4). This evidence, together with aurein 1.2 being only 13 residues in length, indicates that the peptide associates with zwitterionic lipid headgroups in a fashion which propagates part of the way down the hydrophobic acyl chains but itself does not reach significantly beyond the hydrophilic/hydrophobic lipid interface. Aurein 1.2 nevertheless appears to effectively solubilize DMPC bilayers, as mass was lost from the SPR support soon after the increase in mass associated with peptide binding. An alternative possibility, but unlikely at the peptide concentrations used here, is that the peptide may envelope the vesicles, which is consistent with the surface interaction reported by NMR, and lead to their desorption from the chip.

With mixed DMPC/DMPG lipid vesicles, the behavior of aurein 1.2 through all experiments was similar, although generally less dramatic than for the pure DMPC bilayer. With regard to differences in effect on the two lipid components, there may have been slightly more increase in fast DMPG fluctuations than for DMPC (Figure 5), which was likely to be in DMPC-enriched domains (Table 1). Possibly owing to a relatively high proportion of charged residues, while maintaining a side chain charge balance, aurein 1.2 appears to interact with membranes only at the surface with little discrimination between neutral and anionic membrane bilayers (Figures 6 and 7). Similarly, for the related peptides aurein 2.2 and 2.3, little discrimination between anionic and neutral bilayers was seen by oriented circular dichroism and ^{31}P solid-state NMR at lower hydration level (*48*).

Citropin 1.1. Similar to aurein 1.2, but longer and with a more hydrophobic tail, citropin 1.1 may bind at the bilayer surface or partially insert, depending on the lipid system. In pure DMPC vesicles, citropin 1.1 had a strong effect on headgroup dynamics (on the $\sim 10^{-4}$ s time scale) and/or orientation (Table 3), appreciable increase in fluctuations felt at the headgroup on the 10^{-9} and 10^{-3} s time scales (Figure 4), only a slight disordering effect on the CD_2 closest to the bilayer surface, and no effect on the terminal CD_3 (Table 2) on $\sim 10^{-5}$ s time scale. By SPR, citropin 1.1 appeared to bind strongly to DMPC bilayers but did not solubilize appreciable material from the chip at the same concentrations as aurein 1.2.

In mixed bilayers, citropin 1.1 had the strongest effect of any of the peptides on both DMPC and DMPG components with respect to factors influencing headgroup CSA (Table 3) and increased fluctuations felt at the headgroup on the 10^{-9} and 10^{-3} s time scales (Figure 4). The peptide also increased order all along the acyl chain (Table 2, Figure 3). By SPR the binding of citropin 1.1 to mixed bilayers appeared similar to pure DMPC bilayers. Citropin 1.1 would, therefore, appear to bind at the bilayer surface in the absence of DMPG. The binding may be stronger in the presence of DMPG but not in a fashion that segregates the two lipid types within the membrane. Neither lipid system appeared to lose

integrity upon binding of citropin 1.1, which is a longer peptide and has an additional charge compared to aurein.

Maculatin 1.1. With pure DMPC vesicles, maculatin 1.1 behaved similarly to citropin 1.1. Only slight differences were noted, where maculatin appeared to have even less impact on the lipid acyl chains (Table 2), but promoted collective membrane motions on the 10^{-3} s time scale (Figure 4). SPR sensorgrams indicated peptide binding but no significant removal of membrane lipid and in a manner that allowed the peptide to wash away.

The behavior of maculatin 1.1 changed dramatically, however, when DMPG was included in the bilayers. The deuterated DMPC, which was disordered by the presence of DMPG, regained the characteristic order of pure DMPC in the presence of the peptide. Furthermore, fast fluctuations (10^{-9} s time scale) were actually reduced, lengthening T_1 relaxation time for DMPC while fast fluctuations of DMPG were promoted. The SPR sensorgram at lowest concentration indicated binding of maculatin 1.1 to the mixed bilayer surface. Higher concentrations, however, promoted rapid removal of lipid before all peptide was able to bind. Maculatin 1.1 consequently appears to associate with zwitterionic lipid bilayers only at the surface where it is not particularly effective at disrupting membrane integrity. The data using mixed lipids suggest that maculatin has specific affinity for the negative lipid such that the zwitterionic lipid is excluded by default into significantly enriched domains. Although not obvious from the sequence, the combination of this cationic peptide and the appropriate bilayer thickness could lead to domain formation in mixed lipid bilayers. The inability to wash the peptide off at low concentrations and the effect of concentration on binding indicate some cooperativity consistent with a classic two-stage insertion into the membrane followed by formation of an oligomer. While this topology would compromise the membrane without disrupting the bilayer structure *per se*, membrane still appeared to be lost from the mixed lipid system. The slight loss of lipid may indicate multiple modes of interaction in mixed bilayer systems in the presence of excess peptide, leading to some loss of bilayer stability as well as membrane insertion.

Caerin 1.1. Although longer and with a second proline-induced kink in the α-helix, caerin 1.1 behaved similarly to maculatin 1.1 in both lipid systems. The activity profiles observed by SPR, however, differed appreciably. Significantly, the lowest concentration of caerin 1.1 did not bind at all to either lipid system, while the higher concentrations did, but without loss of lipid. Upon the effectual dilution by washing, the higher concentrations of peptide were readily removed from the lipid. These results could be due to some degree of cooperativity, such as peptide oligomerization, which may precede insertion into the membrane, or each peptide affects the membrane structure such that the energy barrier to further insertion by subsequent monomers is lowered. Further work is needed to clarify the nature of the cooperativity, which is more evident with anionic membranes and is consistent with the formation of membrane insertion rather than membrane rupture.

Solid-state NMR revealed that the dynamics of the pure DMPC membranes were most affected by aurein 1.2. Strong interactions between the peptide and the lipid headgroups provide detailed evidence at the molecular level that aurein 1.2 lyses bacterial membranes via a surface interaction consistent with the "carpet" model (*18*). Citropin 1.1, maculatin 1.1, and caerin 1.1 had less effect on the pure DMPC lipid system. T_2 of the maculatin−DMPC sample revealed that maculatin 1.1 had a strong collective effect. Citropin 1.1 had a preference for a net negatively charged environment and strongly affected both the faster and slower motions of the phospholipids. Leakage data (*18*) also suggest that this peptide appears to lyse membranes via a carpet mechanism, but our new evidence indicates that citropin 1.1 may bind parallel to the membrane surface and only partially insert. Monolayer studies (*17*) show that citropin 1.1 and maculatin 1.1 are more miscible with anionic lipids, and calorimetry (*19*) shows that aurein 1.1, citropin 1.1, and maculatin 1.1 interact more strongly with DMPG. Surprisingly, aurein 1.2 did not have as great an effect on mixed bilayers, and maculatin 1.1 and caerin 1.1 may have shown less effect at the membrane surface by NMR due to a transmembrane orientation.

Evidence detailed in our studies is consistent with the earlier phenomenological observations from the leakage of dyes from POPC and POPC/POPG lipid vesicles using aurein 1.2, citropin 1.1, and maculatin 1.1 (*18*). Aurein 1.2 and citropin 1.1 appeared to lyse the model membranes, as encapsulated large dye molecules were released from vesicles at the same time that bilayer structure was lost. The longer peptide, maculatin 1.1, possibly formed pores, as large dyes were retained in the interior of vesicles while small dyes escaped, and overall membrane bilayer integrity was maintained. ATR-FTIR evidence (*49*) further supports the maculatin pore hypothesis. The caerin used in this study is somewhat an extension of maculatin 1.1, being a longer α-helical peptide, with an additional kink due to two prolines versus one. While our present evidence does not necessitate an oligomeric state for the longer peptides, the accumulating information makes the hypothesis of a transmembrane pore increasingly viable. If true, in addition to the β-branched residues, the presence and placement of polar residues may also govern the pore structure, where these residues would point inward toward the aqueous lumen of a pore.

In summary, the results are consistent with a surface interaction for aurein 1.2 and pore formation rather than membrane lysis by the longer peptides. Changes in phospholipid motions and membrane binding information have provided additional insight into the action of AMP. Utilizing both SS-NMR and SPR techniques, further understanding of how antimicrobial peptides interact with bacterial membranes was gained.

REFERENCES

1. Nissen-Meyer, J., and Nes, I. F. (1997) Ribosomally synthesized antimicrobial peptides: their function, structure, biogenesis, and mechanism of action. *Arch. Microbiol. 167*, 67–77.
2. Boman, H. G. (1995) Peptide antibiotics and their role in innate immunity. *Annu. Rev. Immunol. 13*, 91–92.
3. Smet, K., and Contreras, R. (2005) Human antimicrobial peptides: Defensins, cathelicidins and histatins. *Biotechnol. Lett. 27*, 1337–1347.
4. Epand, R. M., Shai, Y. C., Segrest, J. P., and Anantharamaiah, G. M. (1995) Mechanisms for the modulation of membrane bilayer properties by amphipathic helical peptides. *Biopolymers 37*, 319–338.
5. Oren, Z., and Shai, Y. (1998) Mode of action of linear amphipathic α-helical antimicrobial peptides. *Biopolymers 47*, 451–463.
6. Brogden, K. A. (2005) Antimicrobial peptides: pore formers or metabolic inhibitors in bacteria? *Nat. Rev. Microbiol. 3*, 238–250.
7. Bechinger, B. (1997) Structure and functions of channel-forming peptides—magainins, cecropins, melittin and alamethicin. *J. Membr. Biol. 156*, 197–211.

8. Shai, Y. (1999) Mechanism of the binding, insertion and destabilization of phospholipid bilayer membranes by α-helical antimicrobial and cell non-selective membrane-lytic peptides. *Biochim. Biophys. Acta 1462*, 55–70.
9. Yang, L., Harroun, T. A., Weiss, T. M., Ding, L., and Huang, H. W. (2001) Barrel-stave model or toroidal model? A case study on melittin pores. *Biophys. J. 81*, 1475–1485.
10. Lee, M. T., Chen, F. Y., and Huang, H. W. (2004) Energetics of pore formation induced by antimicrobial peptides. *Biochemistry 43*, 3590–3599.
11. Apponyi, M. A., Pukala, T. L., Brinkworth, C. S., Maselli, V. M., Bowie, J. H., Tyler, M. J., Booker, G. W., Wallace, J. C., Carver, J. A., Separovic, F., Doyle, J., and Llewellyn, L. E. (2004) Host-defence peptides of Australian anurans: structure, mechanism of action and evolutionary significance. *Peptides 25*, 1035–1054.
12. Boland, M. P., and Separovic, F. (2006) Membrane interactions of antimicrobial peptides from Australian tree frogs. *Biochim. Biophys. Acta 1758*, 1178–1183.
13. Pukala, T. L., Brinkworth, C. S., Carver, J. A., and Bowie, J. H. (2004) Investigating the importance of the flexible central hinge in caerin 1.1. The solution structures and activities of two synthetically modified peptides. *Biochemistry 43*, 937–944.
14. Marcotte, I., Wegener, K. L., Lam, Y.-H., Chia, B. C. S., De Planque, M. R. R., Bowie, J. H., Auger, M., and Separovic, F. (2003) Interaction of antimicrobial peptides from Australian amphibians with lipid membranes. *Chem. Phys. Lipids 122*, 107–120.
15. Chia, B. C. S., Lam, Y.-H., Dyall-Smith, M., Separovic, F., and Bowie, J. H. (2000) A ^{31}P NMR study of the interaction of amphibian antimicrobial peptides with the membranes of live bacteria. *Lett. Pept. Sci. 7*, 151–156.
16. Balla, M. S., Bowie, J. H., and Separovic, F. (2004) Solid-state NMR study of antimicrobial peptides from Australian frogs in phospholipid membranes. *Eur. Biophys. J. 33*, 109–116.
17. Ambroggio, E. E., Separovic, F., Bowie, J., and Fidelio, G. D. (2004) Surface behaviour and peptide-lipid interactions of the antibiotic peptides, maculatin and citropin. *Biophys. Biochim. Acta 1664*, 31–37.
18. Ambroggio, E. E., Separovic, F., Bowie, J. H., Fidelio, G. D., and Bagatolli, L. A. (2005) Direct visualization of membrane leakage induced by the antibiotic peptides: maculatin, citropin and aurein. *Biophys. J. 89*, 1874–1881.
19. Seto, G. W. J., Marwaha, S., Kobewka, D. M., Lewis, R. N. A. H., Separovic, F., and McElhaney, R. N. (2007) Interactions of the Australian tree frog antimicrobial peptides aurein 1.2, citropin 1.1 and maculatin 1.1 with lipid model membranes: differential scanning calorimetric and Fourier transform infrared spectroscopic studies. *Biochim. Biophys. Acta 1768*, 2787–2800.
20. Mechler, A., Praporski, S., Atmuri, K., Boland, M., Separovic, F., and Martin, L. L. (2007) Antimicrobial peptides from Australian tree frogs interact specifically and selectively with supported phospholipid membranes. *Biophys. J. 93*, 3907–3916.
21. Epand, R. F., Schmitt, M. A., Gellman, S. H., and Epand, R. M. (2006) Role of membrane lipids in the mechanism of bacterial species selective toxicity by two alpha/beta-antimicrobial peptides. *Biochim. Biophys. Acta 1758*, 1343–1350.
22. Hall, K., Mozsolits, H., and Aguilar, M. I. (2003) Surface plasmon resonance analysis of antimicrobial peptide-membrane interactions: affinity and mechanism of action. *Lett. Pept. Sci. 10*, 475–485.
23. Davis, J. H., Jeffrey, K. R., Bloom, M., Valic, M. I., and Higgs, T. P. (1976) Quadrupolar echo deuteron magnetic resonance spectroscopy in ordered hydrocarbon chains. *Chem. Phys. Lett. 42*, 390–394.
24. Pukala, T. L., Boland, M. P., Gehman, J. D., Kuhn-Nentwig, L., Separovic, F., and Bowie, J. H. (2007) Solution structure and interaction of cupiennin 1a, a spider venom peptide, with phospholipid bilayers. *Biochemistry 46*, 3576–3585.
25. Lau, T.-L., Gehman, J. D., Wade, J. D., Perez, K., Masters, C. L., Barnham, K. J., and Separovic, F. (2007) Membrane interactions and the effect of metal ions of the amyloidogenic fragment Aβ(25−35) in comparison to Aβ(1−42). *Biochim. Biophys. Acta 1768*, 2400–2408.
26. Drechsler, A., and Separovic, F. (2003) Solid-state NMR structure determination. *IUBMB Life 55*, 515–523.
27. Dodd, A., and Separovic, F. (2004) An introduction to biological solid state NMR, in *Supramolecular Structure and Function 8* (Pifat-Mrzljak, G., Ed.) pp 145−156, Kluwer Academic/Plenum Publishers, New York.
28. Williams, T., Kelley, C., Lang, R., Kotz, D., Campbell, J., Elber, G., Woo, A., et al. gnuplot, http://www.gnuplot.info.
29. Kamimori, H., Hall, K., Craik, D. J., and Aguilar, M. I. (2005) Studies on the membrane interactions of the cyclotides kalata B1 and kalata B6 on model membrane systems by surface plasmon resonance. *Anal. Biochem. 337*, 149–153.
30. Cornell, B. A., Weir, L. E., and Separovic, F. (1988) The effect of gramicidin A on phospholipid bilayers. *Eur. Biophys. J. 16*, 113–119.
31. Smith, R., Separovic, F., Bennett, F. C., and Cornell, B. A. (1992) Melittin induced changes in lipid multilayers: a solid-state NMR study. *Biophys. J. 63*, 469–474.
32. Seelig, A., and Seelig, J. (1974) The dynamic structure of fatty acyl chains in a phospholipid bilayer measured by deuterium magnetic resonance. *Biochemistry 13*, 4839–4845.
33. Gehman, J. D., and Separovic, F. (2006) Solid-state NMR of membrane-active proteins and peptides, in *Modern Magnetic Resonance Part 1: Applications in Chemistry, Biological and Marine Sciences* (Asakura, T., Saito, H., and Ando, I., Eds.) pp 301−307, Springer, New York.
34. Kohler, S. J., and Klein, M. P. (1977) Orientation and dynamics of phospholipid head groups in bilayers and membranes determined from ^{31}P nuclear magnetic resonance chemical shielding tensors. *Biochemistry 16*, 519–526.
35. Cornell, B. A., and Separovic, F. (1988) A model for gramicidin A−phospholipid interactions in bilayers. *Eur. Biophys. J. 16*, 299–306.
36. Dufourc, E. J., Mayer, C., Stohrer, J., Althoff, G., and Kothe, G. (1992) Dynamics of phosphate head groups in biomembranes. Comprehensive analysis using phosphorus-31 nuclear magnetic resonance lineshape and relaxation time measurements. *Biophys. J. 61*, 42–57.
37. Griffin, R. G., Powers, L., and Pershan, P. S. (1978) Head-group conformation in phospholipids: a phosphorus-31 nuclear magnetic resonance study of oriented monodomain dipalmitoylphosphatidylcholine bilayers. *Biochemistry 17*, 2718–2722.
38. Gehman, J. D., O'Brien, C. C., Shabanpoor, F., Wade, J. D., and Separovic, F. (2008) Metal effects on the membrane interactions of amyloid-β peptides. *Eur. Biophys J. 37*, 333–344.
39. Abragam, A. (1961) *The Principles of Nuclear Magnetism*, p 599, Oxford University Press, Oxford.
40. Cornell, B. A., Hiller, R. G., Raison, J., Separovic, F., Smith, R., Vary, J. C., and Morris, C. (1983) Biological membranes are rich in low frequency motion. *Biochim. Biophys. Acta 732*, 473–478.
41. Separovic, F., Cornell, B., and Pace, R. (2000) Orientation dependence of NMR relaxation time, $T_{1\rho}$, in lipid bilayers. *Chem. Phys. Lipids 107*, 159–167.
42. Mozsolits, H., and Aguilar, M. I. (2002) Surface plasmon resonance spectroscopy: an emerging tool for the study of peptide-membrane interactions. *Biopolymers 66*, 3–18.
43. Chia, X., Carver, J. A., Mulhern, T. D., and Bowie, J. H. (2000) Maculatin 1.1, an antimicrobial peptide from the Australian tree frog. *Eur. J. Biochem. 267*, 1894–1908.
44. Wong, H., Bowie, J. H., and Carver, J. A. (1997) The solution structure and activity of caerin 1.1, an antimicrobial peptide from the Australian green tree frog, *Litoria splendida*. *Eur. J. Biochem. 247*, 545–557.
45. Wegener, K. L., Carver, J. A., and Bowie, J. H. (2003) The solution structures and activity of caerin 1.1 and caerin 1.4 in aqueous trifluoroethanol and dodecylphosphocholine micelles. *Biopolymers 69*, 42–59.
46. Cordes, F. S., Bright, J. N., and Sansom, M. S. P. (2002) Proline-induced distortions of transmembrane helices. *J. Mol. Biol. 323*, 951–960.
47. Senes, A., Gerstein, M., and Engelman, D. M. (2000) Statistical analysis of amino acid patterns in transmembrane helices: the GxxxG motif occurs frequently and in association with β-branched residues at neighboring positions. *J. Mol. Biol. 296*, 921–936.
48. Pan, Y.-L., Cheng, J. T.-J., Hale, J., Pan, J., Hancock, R. E. W., and Straus, S. K. (2007) Characterization of the structure and membrane interaction of the antimicrobial peptides aurein 2.2 and 2.3 from Australian southern bell frogs. *Biophys. J. 92*, 2854–2864.
49. Chia, C. S., Torres, J., Cooper, M. A., Arkin, I. T., and Bowie, J. H. (2002) The orientation of the antibiotic peptide maculatin 1.1 in DMPG and DMPC lipid bilayers. Support for a pore-forming mechanism. *FEBS Lett. 512*, 47–51.

BI800320V